RIBBON 2-KNOTS, 1+1=2, AND DUFLO'S THEOREM FOR ARBITRARY LIE ALGEBRAS

DROR BAR-NATAN, ZSUZSANNA DANCSO, AND NANCY SCHERICH

Abstract. We explain a direct topological proof for the multiplicativity of Duflo isomorphism for arbitrary finite dimensional Lie algebras. The proof follows a series of implications, starting with "the calculation 1+1=2 on a 4D abacus", using the study of *homomorphic expansions* (aka universal finite type invariants) for ribbon 2-knots, and the relationship between the corresponding associated graded space of *arrow diagrams* and universal enveloping algebras. This complements the results of the first author, Le and Thurston, where similar arguments using a "3D abacus" and the Kontsevich Integral was used to deduce Duflo's theorem for *metrized* Lie algebras; and results of the first two authors on finite type invariants of w-knotted objects, which also imply a relation of 2-knots with the Duflo theorem in full generality, though via a lengthier path.

1. Introduction

For a finite dimensional Lie algebra $\mathfrak{g}$, the Duflo isomorphism is an algebra isomorphism $\mathcal{D} : S(\mathfrak{g})^{\mathfrak{g}} \to U(\mathfrak{g})^{\mathfrak{g}}$, where $U(\mathfrak{g})^{\mathfrak{g}}$ and $S(\mathfrak{g})^{\mathfrak{g}}$ are the $\mathfrak{g}$ invariant subspaces for the adjoint action on the universal enveloping algebra and the symmetric algebra. (Recall x is called invariant if $g \cdot x = 0$ for every $g \in \mathfrak{g}$.) The map $\mathcal{D}$ is given by an explicit formula. The difficulty is in showing that this formula represents a homomorphism, namely that it is multiplicative.

This isomorphism was first described for semi-simple Lie algebras by Harish-Chandra in 1951 [HC]. Kirillov conjectured that a formulation of Harish-Chandra's map was an algebra isomorphism for all finite dimensional Lie algebras. Duflo proved Kirillov's conjecture in 1977 [D], and it is now referred to as Duflo's Theorem. Since then, there have been many proofs of Duflo's theorem using techniques outside the setting of the originally formulated problem. For metrized Lie algebras, a topological proof was found by the first author, Le and Thurston in 2009 [BLT] using the Kontsevich integral and a knot theoretic interpretation of "$1+1=2$ on an abacus". In this paper we give a new topological proof of Duflo's theorem for *arbitrary finite dimensional Lie algebras* using a "4-dimensional abacus" instead of an ordinary 3-dimensional one.

The Dulfo isomorphism is also implied by the now-proven Kashiwara–Vergne (KV) conjecture [KV]. The KV conjecture states that a certain set of equations has a solution in the group of *tangential automorphisms* of the degree completed free Lie algebra on 2 generators. One can extract the Duflo isomorphism from such a solution. The KV conjecture was proven by [AM] in 2006 using deformation quantization. New proofs exploiting the relationship between the KV equations and Drinfel'd associators were found by Alekseev, Torossian and Enriquez shortly thereafter [AT, AET]. A topological context and solution in terms of the 4-dimensional knot theory of *w-foams* was established by the first two authors in [BD2, BD3]. In this context, the KV-conjecture is equivalent to the existence of a *homomorphic expansion*

Key words and phrases. knots, 2-knots, tangles, expansions, finite type invariants, Lie algebras, Duflo's theorem .

This work was partially supported by NSERC grant RGPIN 262178 and by ARC DECRA DE170101128.

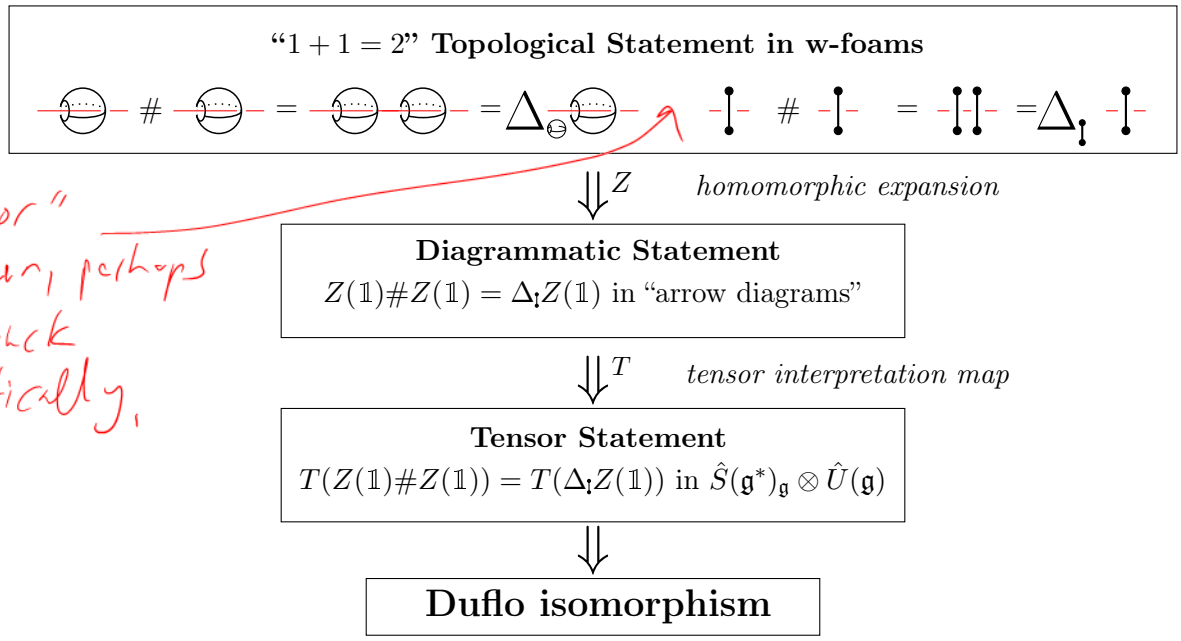

FIGURE 1. The rough sketch of the proof.

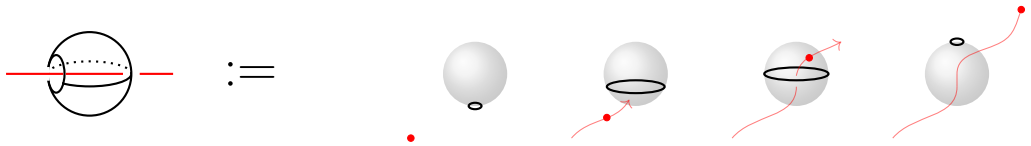

FIGURE 2. The threaded sphere as a movie of a circle and a point in $\mathbb{R}^3$.

for w-foams. In this paper, we directly address how such a homomorphic expansion gives rise to a proof of the multiplicativity of the Duflo isomorphism and a formula for $\mathcal{D}$, and thus completing a topological proof of the Duflo isomorphism in full generality.

This paper is structured to follow the implications shown in the Figure 1. We start with an intuitive topological statement "$1 + 1 = 2$" and interpret this in the more sophisticated setting of w-foams. Using the homomorphic expansion Z and the tensor interpretation map T, we can re-interpret "$1 + 1 = 2$" as an equality in $\hat{S}(\mathfrak{g}^*)_{\mathfrak{g}} \otimes \hat{U}(\mathfrak{g})$. This will imply that our formulation of the Duflo isomorphism is an algebra homomorphism. The essential ingredient in this process is the homomorphic expansion Z of [BD2, BD3].

2. Understanding the Topological Statement and w-foams

2.1. **"4D Abacus Arithmetic".** The "threaded sphere" or "abacus bead" shown in Figure 2 is a knotted object in $\mathbb{R}^4$, and an element of the space of w-foams studied in [BD2]. To understand this 4D object, we describe it as a sequence of 3D slices, or "frames of a 3D movie". The movie starts with two points A and B. Point B opens up to a circle, A flies through the circle, and B closes to a point again. In 4 dimensions this is a line threaded through a sphere with no intersections; and embedded pair. We depict this object as  ; this is a *broken surface diagram* in the sense of [CS].

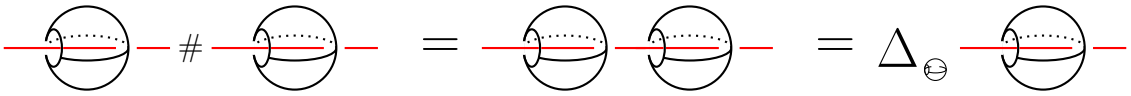

FIGURE 3. "$1+1=2$" on the 4D abacus.

We can interpret "addition on the 4D abacus" by iteratively threading embedded spheres on a single thread, or in other words, connecting along the threads, as shown in Figure 3. There are two ways to obtain the number 2 from the number 1: by addition – which is represented by iterative threading on the "abacus" thread as above, or by doubling, as explained below.

Assuming the sphere is equipped with a normal vector field (a.k.a. framing, and we will define such a framing later), it makes sense to double the sphere along its framing. This operation will be denoted by $\Delta_{\ominus}$  . For example, given the outward-pointing normal vector field, doubling the sphere results in two concentric spheres. In $\mathbb{R}^4$ two concentric spheres can be separated without intersecting each other. E.g, assume the coordinates are called x, y, z and t, and two concentric spheres lie in the hyperplane $\{z=0\}$. Then one can continuously move the inner sphere into the hyperplane $z=1$, followed by moving it to a disjoint t-position from the outer sphere and then back to the $\{z=0\}$ hyperplane. Combining this with threading, we obtain that doubling a threaded sphere has the same effect as the connected sum of two threaded spheres, as shown in Figure 3. To simplify notation, we will denote the threaded sphere by $\mathbb{1}$, and write $\mathbb{1}\#\mathbb{1} = \Delta_{\ominus}\mathbb{1}$.

2.2. **w-Foams.** In order to introduce the main ingredient Z, the homomorphic expansion, we need to place the threaded sphere in the more complex space of w-foams. We will briefly describe this space here and for more detail refer to [BD3, Section 2].

The space of w-foams, denoted $\widetilde{wTF}$, is a *circuit algebra*, as defined in [BD2, Section 2.4]. In short, circuit algebras are similar to the planar algebras of Jones [J] but without the planarity requirement for the connection diagrams. For an example of a circuit algebra connection diagram, see Figure 6. Circuit algebras are also close relatives of modular operads. Each generator and relation of $\widetilde{wTF}$ has a local topological interpretation in terms of certain *ribbon knotted tubes with foam vertices and strings* in $\mathbb{R}^4$. Note that one dimensional strands cannot be knotted in $\mathbb{R}^4$, however, they can be knotted *with* two-dimensional tubes. In the diagrams, two-dimensional tubes will be denoted by **thick lines** and one dimensional strings by thin red lines.

With this in mind, we define $\widetilde{wTF}$ as a circuit algebra given in terms of generators and relations, and with some extra operations beyond circuit algebra composition. The generators, relations and operations are explained in detail in Sections 2.2.1 and 2.2.2. The local topological interpretation of the generators and relations provides much of the intuition for this paper.

$$\widetilde{wTF} = CA\left\langle \underbrace{1\ ,\ 2\ ,3,\ 4\ ,\ 5\ ,\ 6\ ,\ 7\ ,\ 8\ ,\ 9}_{\text{generators}} \,\middle|\, \underbrace{R1^s\ ,\ R2,\ R3,\ R4,\ OC,\ CP}_{\text{relations}} \,\middle|\, \underbrace{u_e}_{\text{extra operation}} \right\rangle$$

In [BD3] $\widetilde{wTF}$ appears in its larger unoriented version (includes a *wen* and relations describing its behaviour) and it is equipped with more auxiliary operations (eg punctures, orientation

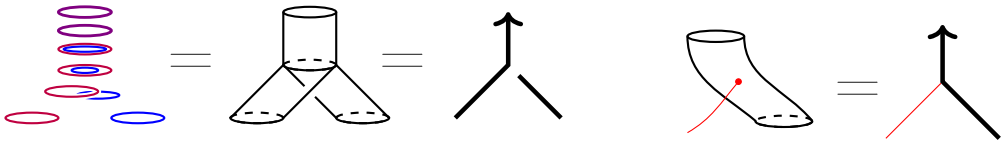

FIGURE 4. The trivalent vertices of $\widetilde{wTF}$.

switches). The expansion Z constructed there is *homomorphic* with respect to all of the operations in the appropriate sense. Here we focus only on orientable surfaces and the operations strictly needed for the Duflo isomorphism – the restriction of the Z of [BD3] is a homomorphic expansion for this structure. In the following sections we will provide brief descriptions of $\widetilde{wTF}$, its associated graded space of arrow diagrams, and the homomorphic expansion, to make this paper more self-contained.

2.2.1. *The generators of* $\widetilde{wTF}$. We begin by discussing the local topological meaning of each generator shown above. For more details, see [BD2, Sections 4.1.1 and 4.5]

Knotted (more precisely, braided) tubes in $\mathbb{R}^4$ can equivalently be thought of as movies of flying circles in $\mathbb{R}^3$. The two crossings – generators 1 and 2 – stand for movies where two circles trade places as the circle corresponding to the under strand flies through the circle corresponding to the over strand entering from below. The bulleted end in generator 3 represents a tube "capped off" by a disk, or alternatively the movie where a circle shrinks to a point and disappears.

Generators 4 and 5 stand for singular "foam vertices", and will be referred to as the positive and negative vertex, respectively. The positive vertex represents the movie shown in Figure 4: the right circle approaches the left circle from below, flies inside it and merges with it. The negative vertex represents a circle splitting and the inner circle flying out below and to the right.

The thin red strands denote one dimensional strings in $\mathbb{R}^4$, or "flying points in $\mathbb{R}^3$". The crossings between the two types of strands (generators 6 and 7) represent "points flying through circles". For example, generator 6  stands for "the point on the right approaches the circle on the left from below, flies through the circle and out to the left above it". This explains why there are no generators with a thick strand crossing under a thin red strand: a circle cannot fly through a point.

Generator 8 is a trivalent vertex of 1-dimensional strings in $\mathbb{R}^4$. Finally, generator 9 is a "mixed vertex", in other words a one-dimensional string attached to the wall of a 2-dimensional tube. This is shown in Figure 4.

An important notion for later use is the *skeleton* of a w-foam. We give an intuitive definition here that is is sufficient for this paper; for a formal definition see [BD2, Section 2.4]. In general, viewing knotted objects as embeddings of circles, manifolds, graphs, etc, the skeleton is the embedded object without its embedding. In other words, the skeleton of a knotted object is obtained by allowing arbitrary crossing changes, or equivalently by replacing all crossings with "virtual" (or circuit) crossings. For example, the skeleton of an ordinary knot is a circle. The skeleton of the threaded sphere described above is a sphere and a string. The skeleton of a classical braid on n strands is an element of the permutation group S_n.

2.2.2. *The relations for* $\widetilde{wTF}$. This section is a quick overview of the relations for $\widetilde{wTF}$, which are described in detail in [BD2, Section 4.5]. The list of relations for $\widetilde{wTF}$ is {R1^s, R2, R3, R4,

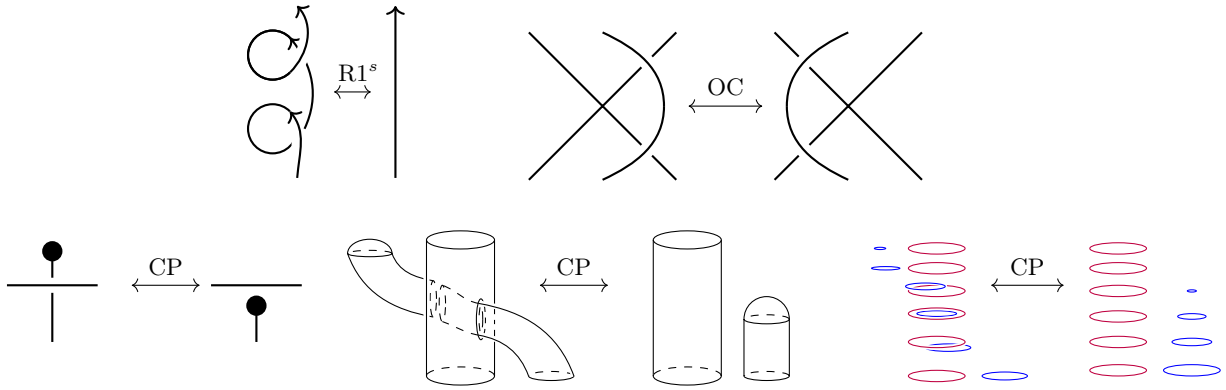

FIGURE 5. The relations $R1^s$ and OC are shown. CP is explained with broken surface diagrams and as a movie of flying circles.

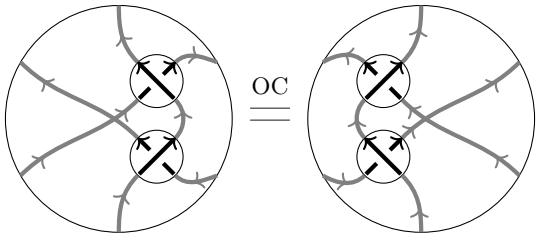

FIGURE 6. The OC relation written as a circuit algebra relation between two crossings.

OC, CP}; Figure 5 shows R1^s and OC, and explains CP. All relations have local 4-dimensional topological meaning, this is an instructive exercise to verify. R1^s stands for the weak (framed) version of the Reidemeister 1 move; R2 and R3 are the usual Reidemeister moves; and R4 allows moving a strand over or under a vertex. OC stands for *Over-corssings Commute*, and CP for *Cap Pullout*. All relations should be interpreted in all sensible combinations of strand types: tube or string, and all orientations.

Note that all relations are circuit algebra relations. For example, the relation OC is understood as a relationship between two specific circuit diagram compositions of  and  , as shown in Figure 6.

The circuit algebra $\widetilde{wTF}$ is conjectured to be a Reidemeister theory for *ribbon* knotted tubes in $\mathbb{R}^4$ with caps, singular foam vertices and strings. Here *ribbon* means that the tubes have "filling" in $\mathbb{R}^4$ with only restricted types of singularities, for details see [BD1, Section 2.2.2]. All the relations represent local topological statements: for example, Reidemeister 2 with a thin red bottom strand holds because the movie consisting of a point flying in through a circle and then immediately flying back out is isotopic to the movie in which the point and circle stay in place. However, it is an open question whether the known relations are sufficient. A similar Reidemeister theory has been proven for w-braids,which exhibits a simpler structure than $\widetilde{wTF}$: [BH, Proposition 3.3] and [Gol,Sa]. For an explanation of the difficulties that arise for knots and tangles, see [BD2, Introduction].

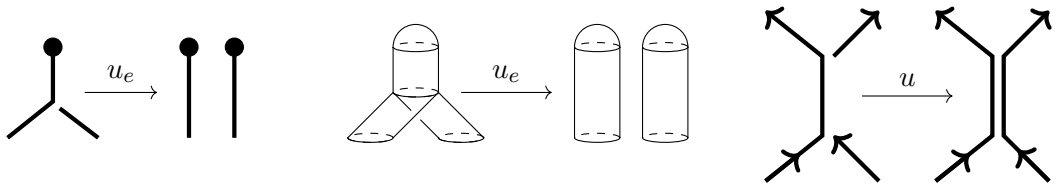

FIGURE 7. Disc unzip on the left and middle, strand unzip on the right.

2.2.3. *The operations on* $\widetilde{wTF}$. In addition to the circuit algebra structure, $\widetilde{wTF}$ is equipped with a set of auxiliary operations. Of these, in this paper we only use *disc unzip*.

The *disc unzip operation* u_e is defined for a capped strand labeled by e. Using the blackboard framing, u_e doubles the capped strand e and then attaches the ends of the doubled strand to the connecting ones, as shown Figure 7.

Topologically, the blackboard framing of the diagram induces a framing of the corresponding tubes and discs in $\mathbb{R}^4$ via Satoh's tubing map [BD1, Section 3.1.1] and [Sa]. Briefly, each point of a (thick black) strand represents a circle in $\mathbb{R}^4$ via the tubing map, and the blackboard framing induces a "companion circle" (not linked with the original circle). A framed tube in $\mathbb{R}^4$ can be understood as a movie of flying circles in $\mathbb{R}^4$ with companions. Unzip is the operation "pushing each circle off of itself slightly in the direction of the companion circles". See also [BD2, Section 4.1.3] for details on framings and unzips.

A related operation not strictly necessary for this paper, *strand unzip*, is defined for strands which end in two vertices of opposite signs, as shown in the right of Figure 7. For the interested reader a detailed definition of crossing and vertex signs is in [BD2, Sections 3.4 and 4.1]. Strand unzip doubles the strand in the direction of the blackboard framing, and connects the ends of the doubled strands to the corresponding edge strands. Topologically, strand unzip pushes the tube off in the direction of the blackboard framing, as before.

2.3. **Interpreting "1 + 1 = 2" in w-foams.** The threaded sphere of Section 2.1 can be described in $\widetilde{wTF}$ by the diagram , since a doubly capped tube is in fact a sphere. Recall that the "4D abacus" interpretation of "1 + 1 = 2" is $\mathbb{1}\#\mathbb{1} = \Delta_!\mathbb{1}$, where $\mathbb{1}$ is the threaded sphere, and $\Delta_!$ is the doubling of the sphere along a framing.

The connected sum # operation for the threaded sphere is the circuit algebra composition shown in Figure 8. Doubling strands is realized in $\widetilde{wTF}$ using the unzip operation. However, since the unzip operations in $\widetilde{wTF}$ require an unzipped strand to end in either a vertex and a cap, or two vertices, we need to define a new *sphere unzip* operation, which doubles a twice-capped strand) along the blackboard framing, also shown in Figure 8. In Section 3 we will need to show that the *homomorphic expansion* of $\widetilde{wTF}$ also respects this operation. To summarize, the topological statement "1 + 1 = 2" expressed in $\widetilde{wTF}$ is shown in Figure 9.

3. Understanding the Diagramatic Statement

3.1. **The associated graded structure** $\mathcal{A}^{sw}$**.** As in [BD3], the structure $\widetilde{wTF}$ is filtered by powers of its augmentation ideal and its associated graded structure, denoted $\mathcal{A}^{sw}$, is a space of *arrow diagrams on foam skeleta*. The *arrows* are drawn as black dotted oriented lines, and the skeleton w-foam elements are drawn with the usual thick black lines and thin red lines. Just like $\widetilde{wTF}$, $\mathcal{A}^{sw}$ is a circuit algebra presented in terms of generators and relations

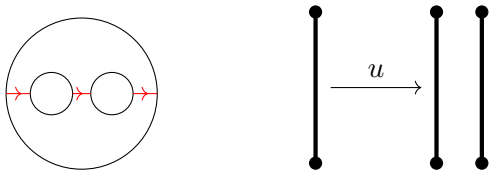

FIGURE 8. On the left, the circuit connection diagram for the connect sum operation, or concatenating along the red strings. On the right, the sphere unzip operation.

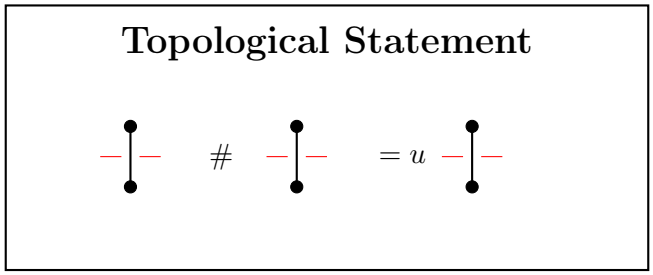

FIGURE 9. The topological statement in w-foams: the connected sum of two threaded spheres along the threads is the same as the sphere unzip of a threaded sphere.

as follows:

$$\mathcal{A}^{sw} = CA\left\langle \underset{1}{\uparrow\cdots\uparrow}, \underset{2}{\uparrow}, \underset{3}{\curlyvee}, \underset{4}{\curlywedge}, \underset{5}{\uparrow\cdots\uparrow}, \underset{6}{\curlyvee}, \underset{7}{\curlywedge} \,\middle|\, RI, CP, \overrightarrow{4T}, \overrightarrow{VI}, TC \,\middle|\, u_e \right\rangle.$$

Generators 1 and 5 are *single arrows*. A single arrow is a degree 1 element of the associated graded space and represents the difference of a crossing and a non-crossing. The arrow head lies on the under (fly-through) strand of the crossing, and the tail lies on the over strand. All of the other generators of $\mathcal{A}^{sw}$ are *skeleton features* of degree zero. Note that the generators don't include any arrow tails on a red string: the topological reason for this is that red strings never cross over any other strand.[1] The relations of $\mathcal{A}^{sw}$ are briefly described below, see [BD2, Section 4.2.1] for more detail.

The RI (Rotation Invariance) relation is a consequence of $R1^s$, and CP is the diagrammatic analogue of the CP relation for $\widetilde{wTF}$. Both are shown in Figure 10. The $\overrightarrow{4T}$ and $\overrightarrow{VI}$ relations are also shown in Figure 10. In both cases the ambiguous strands can be either thick black or thin red, but must be consistent through the relation. The $\overrightarrow{VI}$ relation is the diagrammatic analogue of $R4$, and $4T$ has a slightly more complicated topological explanation. The TC (Tails Commute) relation is a consequence of OC and shown in Figure 11.

This presentation of $\mathcal{A}^{sw}$ is intuitive as a mirror of the circuit algebra presentation of $\widetilde{wTF}$. However, for relating $\mathcal{A}^{sw}$ to Lie algebras, it is more useful to use the following isomorphic formulation in terms of *w-Jacobi diagrams*.

[1]Alternatively, we could introduce a relation asserting that arrow tails on red strings equal zero. This is necessary in [BD3] because a 'puncture' operation can give rise to a diagram with a tail on a red string, but not necessary here.

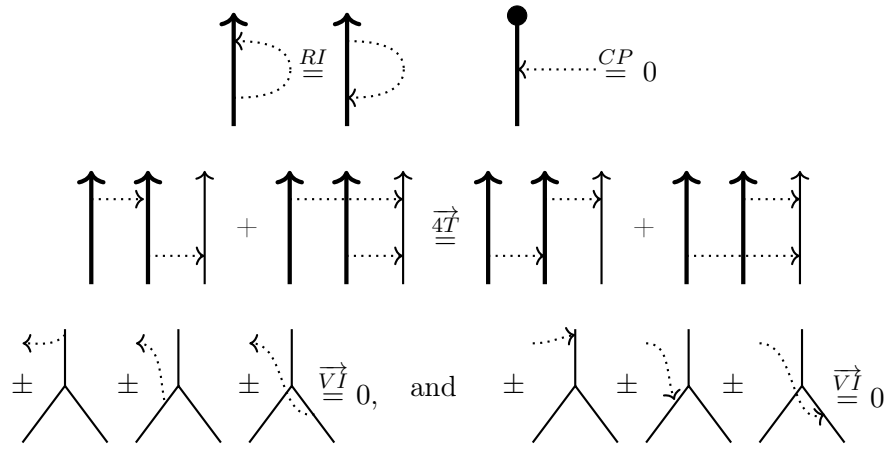

FIGURE 10. The relations RI, CP, $\overrightarrow{4T}$ and $\overrightarrow{VI}$. In the $\overrightarrow{VI}$ relation, signs are positive when the strand of the arrow ending is oriented towards the vertex, and negative otherwise.

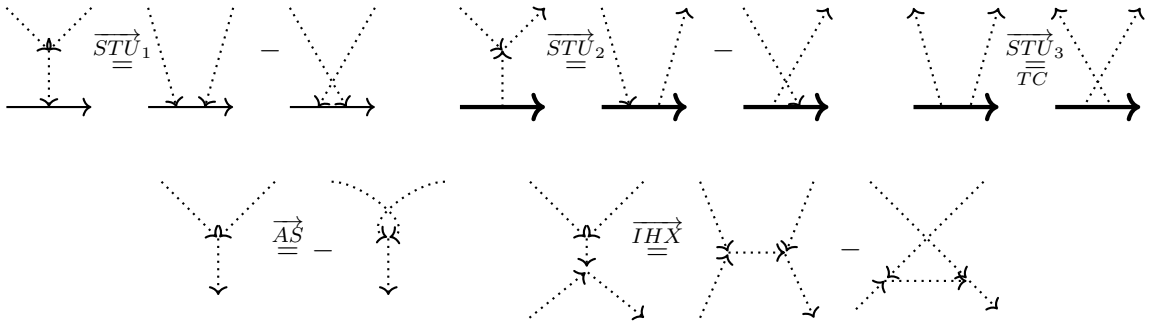

FIGURE 11. The relations $\overrightarrow{STU}$, $\overrightarrow{AS}$ and $\overrightarrow{IHX}$ on $\mathcal{A}^{swt}$.

A *w-Jacobi diagram* consist of a $\widetilde{wTF}$ skeleton and 'arrow graphs' between the components of the skeleton. An *arrow graph* is an oriented uni-trivalent graph, with the following three properties:

(1) Univalent vertices are attached to the skeleton.
(2) Trivalent vertices are equipped with a cyclic orientation.
(3) The edges are oriented so that every trivalent vertex has two 'in' arrows and one 'out' arrow. This is referred to as the *2-in-1-out* property.

Let $\mathcal{A}^{swt}$ denote the circuit algebra of linear combinations of w-Jacobi diagrams modulo the relations $\overrightarrow{STU}$, CP, RI and $\overrightarrow{VI}$ relations. The $\overrightarrow{STU}$ relation (really three relations) is shown in Figure 11, with TC (Tails Commute) being a degenerate case. The $\overrightarrow{AS}$ and $\overrightarrow{IHX}$ relations, also shown in Figure 11, are consequences of $\overrightarrow{STU}$, and so is $\overrightarrow{4T}$. Once again, ambiguous strands can be either thick black or thin red, consistently throughout the relation. The following theorem is the arrow diagram analogue of a well-known fact about classical "chord diagrams":

Theorem 3.1. *[BD2, Theorem 3.8] The obvious inclusion $\mathcal{A}^{sw} \to \mathcal{A}^{swt}$ is a circuit algebra isomorphism.*

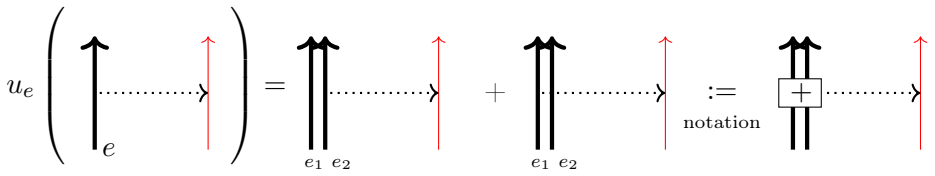

FIGURE 12. Unzipping the strand labeled e, where e_1 and e_2 are the two new strands replacing e.

In light of this we drop the t superscript and write $\mathcal{A}^{sw}$ to denote the space of Jacobi diagrams. The advantage of Jacobi diagrams is that trivalent vertices satisfy the same properties as a Lie bracket—this will be made precise using the tensor interpretation map in Section 4.1.

We introduce the following notation: For a w-foam $F \in \widetilde{wTF}$, the circuit algebra $\mathcal{A}^{sw}(S(F))$ is the space of Jacobi diagrams with skeleton $S(F)$, where $S(F)$ is the skeleton of F as defined in Section 2.2. Often we will write $\mathcal{A}^{sw}(F)$ to mean $\mathcal{A}^{sw}(S(F))$.

The associated graded operation of the circuit algebra composition in $\widetilde{wTF}$ is the circuit algebra composition in $\mathcal{A}^{sw}$. As for the (strand, disc and sphere) unzip operations u_e, given a w-foam F with a choice of a strand e, the associated graded unzip operation $u_e : \mathcal{A}^{sw}(F) \to \mathcal{A}^{sw}(u_e(F))$ maps each arrow ending on e to a sum of two arrows, one ending on each of the two new strands which replace e. For example, an arrow diagram with k arrows ending on e – either heads or tails – is mapped to a sum of 2^k arrow diagrams. This sum is represented notationally as shown in Figure 12.

3.2. **The Homomorphic Expansion.** As proved by the first two authors in [BD2, BD3], there exists a (group-like) *homomorphic expansion* $Z : \widetilde{wTF} \to \mathcal{A}^{sw}$. An expansion is a filtered linear map with the property that the associated graded map $\operatorname{gr} Z : \mathcal{A}^{sw} \to \mathcal{A}^{sw}$ is the identity map on $\mathcal{A}^{sw}$. A homomorphic expansion is an expansion that is a circuit algebra homomorphism and also intertwines each auxiliary operation (here only unzip) of $\widetilde{wTF}$ with its arrow diagrammatic counterpart, meaning that the square below commutes. For disc unzip, this was shown in [BD2, BD3]; for sphere unzip, we will prove it in Lemma 3.4.

$$\begin{array}{ccc} \widetilde{wTF} & \xrightarrow[u_e]{} & \widetilde{wTF} \\ Z \downarrow & & \downarrow Z \\ \mathcal{A}^{sw} & \xrightarrow[u_e]{} & \mathcal{A}^{sw} \end{array}$$

The map Z sends each generator G to an infinite sum of arrow diagrams on the skeleton $S(G)$, that is, $Z(G) \in \mathcal{A}^{sw}(S(G))$. The values of the crossings and the cap are computed explicitly in [BD2,BD3]; to refer to them we use the notation shown in Figure 13. In particular, the Z-value of a crossing of a black strand and a red string is the exponential e^a of an arrow a, to be interpreted as the power series, where a^n is shown in Figure 13.

To describe the Z-value C of a cap, we need to introduce a special class of arrow diagrams called *wheels*. A wheel is an oriented cycle of arrows with a finite number of incoming arrows, or "spokes". (The 2-in-1-out property forces that all univalent ends of this arrow graph be arrow tails, that is, all spokes are incoming.) See Figure 18 for an example of a wheel. Note

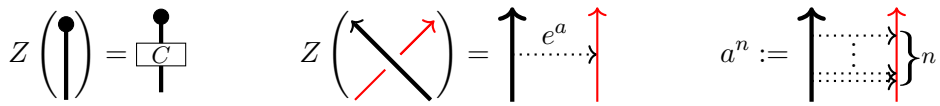

FIGURE 13. Values of Z on generating w-foams.

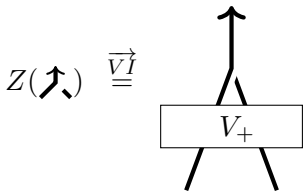

FIGURE 14. The definition of V_+.

that reversing the orientation of an even wheel yields an equivalent arrow diagram via $\overrightarrow{AS}$ and TC relations, while reversing the orientation of an odd wheel produces its negative. Hence, from now on we assume all wheels are oriented clockwise. The value C is an infinite sum of even wheels:

$$C = \exp\left(\sum_{n=1}^{\infty} c_{2n} w_{2n}\right), \quad \text{where} \quad \sum_{n=1}^{\infty} c_{2n} x^{2n} = \frac{1}{4}\log\frac{\sinh x/2}{x/2}. \tag{3.1}$$

In particular, $c_2 = \frac{1}{96}$, $c_4 = -\frac{1}{11520}$, and $c_6 = \frac{1}{752776}$.

Since Z is a circuit algebra homomorphism, given the values of Z on the generators, it is straightforward to compute Z of any w-foam F: if F is a circuit composition of some generators $\{G_i\}$, then $Z(F)$ is the same circuit composition of the values $Z(G_i)$.

We are working towards a diagrammatic statement of "$1 + 1 = 2$", which depends heavily on the homomorphicity of Z. We have yet to prove that Z is homomorphic with respect to the sphere unzip operation, and to achieve this we need to discuss the Z-values of the vertices in some detail. By definition, $Z($ $) \in \mathcal{A}^{sw}($ $)$. Using iterative applications of the relation $\overrightarrow{VI}$, all arrow endings on the vertical strand of $Z($ $)$ can be moved to the bottom two strands. This induces an isomorphism $\mathcal{A}^{sw}($ $) \cong \mathcal{A}^{sw}($ $)$ [BD2]. Thus, $Z($ $)$ can be viewed as an element of $\mathcal{A}^{sw}($ $)$ denoted by V_+, as shown in Figure 14. The arrow diagram $V_- = Z($ $) \in \mathcal{A}^{sw}($ $)$ is defined similarly.

Note that $\mathcal{A}^{sw}($ $)$ is an algebra[2] with multiplication given by vertical concatenation. Let us recall a useful fact from [BD2]:

Lemma 3.2. *In $\mathcal{A}^{sw}($ $)$, V_+ and V_- are multiplicative inverses, i.e. $V_+ \cdot V_- = 1 =$* $\mathcal{A}^{sw}($ $)$.

Proof. This follows from the fact that Z is homomorphic with respect to the unzip operation, as shown in Figure 15. □

The following corollary is a crucial ingredient in proving that Z is also homomorphic with respect to sphere unzip:

[2]In fact, a Hopf algebra with coproduct $\square : \mathcal{A}^{sw}($ $) \to \mathcal{A}^{sw}($ $) \otimes \mathcal{A}^{sw}($ $)$. The coproduct $\square$ of an arrow diagram is a sum of all possible ways of attaching each of the connected component of the arrow graph – after removing the skeleton – to one of the tensor factor skeleta. Details on the Hopf algebra structure are in [BD2, Section 3.2].

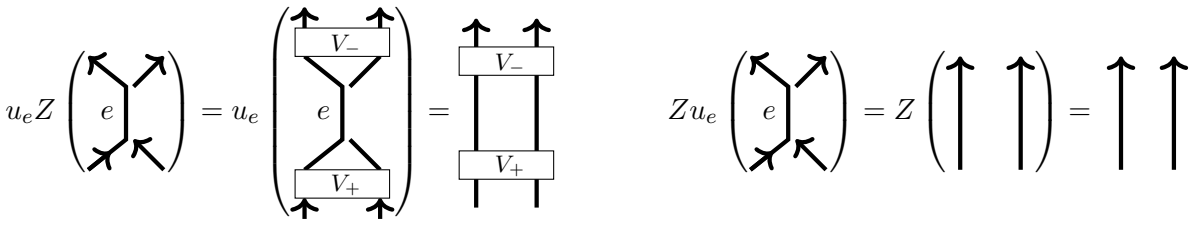

FIGURE 15. Visual proof of Lemma 3.2.

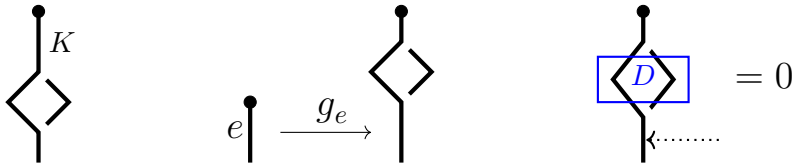

FIGURE 16. The "cactus" w-foam K on the left, cactus grafting in the middle. The "head invariance" property of arrow diagrams on K is shown on the right, where D denotes any arrow diagram above the arrow head on the skeleton K.

Corollary 3.3. $Z(\diamond) = \diamond$, *that is, the Z-value of this w-foam is trivial, a skeleton with no arrows.* □

Lemma 3.4. *Any homomorphic expansion Z of $\widetilde{wTF}$ is also homomorphic with respect to sphere unzip.*

Proof. To prove this we realize the sphere unzip operation as a composition of disc unzips with another new operation called "cactus grafting". Let K denote the "cactus" w-foam shown in Figure 16. If e is a capped strand of a w-foam, the *cactus grafting* operation g_e attaches K to the capped end of e. This is well-defined: the only relation involving a cap is CP, namely, the cap can be pulled out from under a strand. The same is true for the cactus, combining CP with $R4$ moves. Topologically, cactus grafting is cutting a small disk out of a capped strand and gluing the resulting boundary circle to the boundary of the cactus K.

The associated graded cactus grafting operation on arrow diagrams – also denoted g_e – simply attaches the skeleton K (without any arrows) at the end of the capped strand e in place of the cap. This is well-defined: the cap participates only in the CP relation, that is, an arrow head that is not separated from the cap by another arrow ending is zero. However, an arrow head on K that is not separated by another arrow ending from the bottom of K is also zero, as shown in Figure 16; this property is known as the *head invariance of arrow diagrams* [BD2, Remark 3.14].

Finally, Corollary 3.3 implies that $Z(K)$ is simply a cap value C at the top of an otherwise empty skeleton K. Since the value C can be move from the top to the bottom of K using two $\overrightarrow{VI}$ relations, we obtain that for any w-foam F with a capped edge e, $Z(g_e(F)) = g_e(Z(F))$, in other words Z is homomorphic with respect to g_e.

Finally, sphere unzip can be written as a composition of one cactus grafting followed by two disc unzips, hence Z is homomorphic with respect to sphere unzip. □

3.3. **The diagrammatic statement.** Applying the homomorphic expansion Z to the topological statement of Section 2.3 gives rise to the following equation:

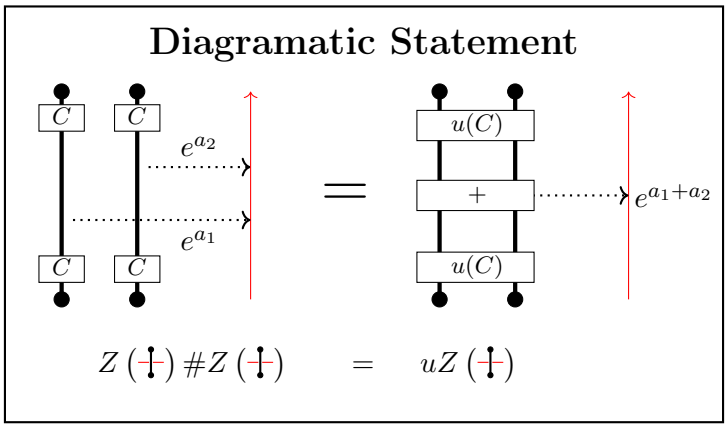

FIGURE 17. The Diagrammatic Statement of "1 + 1 = 2" in $\mathcal{A}^{sw}$. Since tails commute, two caps on a strand can be combined into C^2, and the two unzipped caps can be combined as $u(C)^2 = u(C^2)$.

$$Z(\cdot\cdot) = Z(\cdot)\#Z(\cdot) = uZ(\cdot)$$

Using the notation of Figure 13, we can compute each term of this individually to obtain the final form of the diagrammatic statement, as shown in Figure 17.

4. Understanding the Tensor Statement

Ultimately we aim to give a proof of the multiplicativity of the Duflo isomorphism, which is a statement about finite dimensional Lie algebras. From here on, we fix a finite dimensional Lie algebra $\mathfrak{g}$ over a field $\mathbb{K}$ of characteristic zero. Let $I\mathfrak{g}$ denote the *double* of $\mathfrak{g}$, that is, the semidirect product $\mathfrak{g}^* \rtimes \mathfrak{g}$, where $\mathfrak{g}^*$ is taken to be abelian, and $\mathfrak{g}$ acts on $\mathfrak{g}^*$ by the coadjoint action. In formulae:

$$I\mathfrak{g} = \{(\varphi, x) : \varphi \in \mathfrak{g}^*, x \in \mathfrak{g}\},$$

$$[(\varphi_1, x_1), (\varphi_2, x_2)] = (x_1 \cdot \varphi_2 - x_2 \cdot \varphi_1, [x_1, x_2]). \tag{4.1}$$

We define the *tensor interpretation* map

$$T : \mathcal{A}^w(\uparrow^n) \to (U(I\mathfrak{g})^{\otimes n})^\wedge,$$

where $A^w(\uparrow^n)$ denotes arrow diagrams on n thick black strands, modulo the three $\overrightarrow{STU}$ relations only[3]. $U(I\mathfrak{g})$ is the universal enveloping algebra of $I\mathfrak{g}$, and $^\wedge$ denotes the degree completion, where elements of $\mathfrak{g}^*$ are defined to be degree 1, and elements of $\mathfrak{g}$ are degree zero. We will show that when $n = k_1 + k_2$, T descends to a map

$$T : \mathcal{A}^{sw}(\overset{k_1}{\bullet}\uparrow\overset{k_2}{\uparrow}) \to (S(\mathfrak{g}^*)^{\otimes k_1}_{\mathfrak{g}} \otimes U(\mathfrak{g})^{\otimes k_2})^\wedge.$$

Here $\mathcal{A}^{sw}(\overset{k_1}{\bullet}\uparrow\overset{k_2}{\uparrow})$ is the space of arrow diagrams on the skeleton of k_1 spheres and k_2 strings (see Figure 18 for examples) modulo all three $\overrightarrow{STU}$ relations, as well as CP at both ends of the capped strands, as in Section 3. Note that the RI relation is vacuous on red strings, and it follows from the CP relation on the twice-capped strands: short arrows can be commuted to the cap they point towards, hence they vanish. $S(\mathfrak{g}^*)$ is the symmetric algebra of the linear

[3]It would be called $\mathcal{A}^{sw}(\uparrow^n)$ if we also imposed RI.

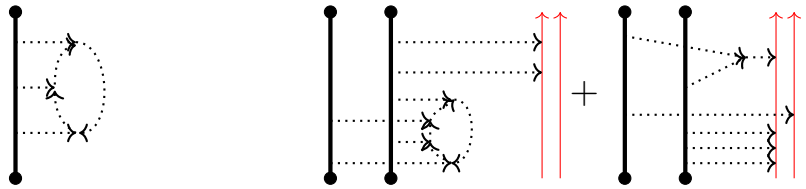

FIGURE 18. An wheel with three spokes in $\mathcal{A}^{sw}(\uparrow^1\uparrow^0)$, and an element in $\mathcal{A}^{sw}(\uparrow^2\uparrow^2)$.

dual of $\mathfrak{g}$, and the subscript $\mathfrak{g}$ denotes co-invariants under the co-adjoint action of $\mathfrak{g}$: that is, the quotient by the image of the co-adjoint action. $U(\mathfrak{g})$ is the universal enveloping algebra of $\mathfrak{g}$, and $\hat{}$ denotes the degree completion where elements of $\mathfrak{g}^*$ are degree one and elements of $\mathfrak{g}$ are degree zero, as before.

4.1. **The Tensor Intpretation Map.** The idea in the construction of $T : \mathcal{A}^w(\uparrow^n) \to (U(I\mathfrak{g})^{\otimes n})\hat{}$ is that trivalent arrow vertices "represent" the Lie bracket in $\mathfrak{g}$, and the relations in $\mathcal{A}^{sw}(\uparrow^n)$ translate to Lie algebra axioms.

Denote the structure tensor of the Lie bracket of $\mathfrak{g}$ by $[,]_\mathfrak{g} \in \mathfrak{g}^* \otimes \mathfrak{g}^* \otimes \mathfrak{g}$. Given a basis $\{b_1, \cdots, b_m\}$ for $\mathfrak{g}$ and the dual basis $\{b_1^*, \cdots, b_m^*\}$ for $\mathfrak{g}^*$, write $[b_i, b_j] = \sum_{k=1}^m c_{ij}^k b_k$ for structure constants $c_{ij}^k \in \mathbb{K}$. Then

$$[,]_\mathfrak{g} = \sum_{i=1}^n c_{ij}^k \, b_i^* \otimes b_j^* \otimes b_k.$$

Similarly, let $\mathrm{id} \in \mathfrak{g}^* \otimes \mathfrak{g}$ denote the identity tensor, given by $\mathrm{id} = \sum_{i=1}^m b_i^* \otimes b_i$.

For an arrow diagram D we first define $T(D)$ in the tensor algebra $\mathcal{T}(I\mathfrak{g})^{\otimes n}$ as follows, and as shown in Figure 19:

(1) Place a copy of $\mathrm{id} \in \mathfrak{g}^* \otimes \mathfrak{g}$ on every single arrow, with $\mathfrak{g}^*$ at the arrow tail, and $\mathfrak{g}$ at the arrow head.
(2) Place the structure tensor of the bracket $[,]_\mathfrak{g}$ on all trivalent arrow vertices, with $\mathfrak{g}^*$ components on the incoming arrows and the $\mathfrak{g}$ component at the outgoing arrow.
(3) Arrows which connect two trivalent vertices now have an element of $\mathfrak{g}^*$ meeting an element of $\mathfrak{g}$. Contract these by evaluating the element of $\mathfrak{g}^*$ on the element of $\mathfrak{g}$ to get a coefficient in $\mathbb{K}$. Multiply the constants together. This is illustrated on examples in Figures 20 and 21.
(4) What remains is a linear combination of diagrams with elements of $\mathfrak{g}^*$ and $\mathfrak{g}$ along the strands. Multiplying these in $\mathcal{T}(I\mathfrak{g})$ along the orientation of the strands produces an element in $\mathcal{T}I\mathfrak{g}^{\otimes n}$.

Given the bases $\{b_1, ..., b_m\}$ for $\mathfrak{g}$ and $\{b_1^*, ..., b_m^*\}$ for $\mathfrak{g}^*$, a simple way to compute the value of T on a given diagram D is to some over all ways of labelling each arrow with an index $1, ..., m$, form the corresponding product in $\mathcal{T}(I\mathfrak{g})^{\otimes n}$ taking a factor b_i for each arrow tail labelled i and b_j^* for each arrow head labelled j; with the coefficient given by the product of c_{rs}^t for each arrow vertex with incoming arrows labelled r and s and outgoing arrow labelled t. See Figures 20 and 21 for sample computations of T for two arrow diagrams.

Lemma 4.1. *T descends to a well defined map on $\mathcal{A}^w(\uparrow^n) \to (U(I\mathfrak{g})^{\otimes n})\hat{}$.*

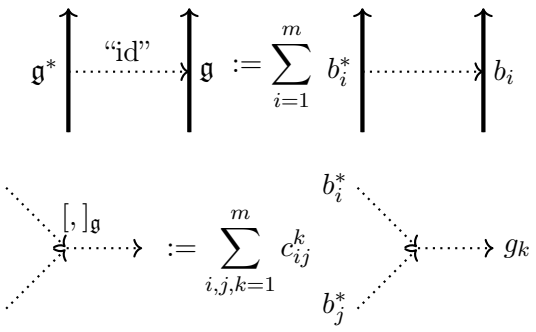

FIGURE 19. Steps (1) and (2) in computing T.

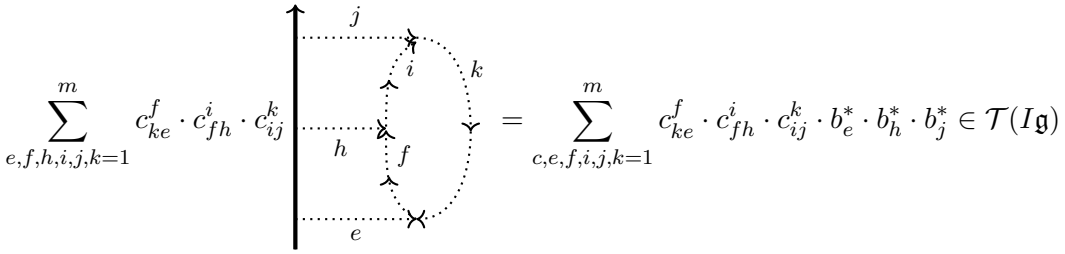

FIGURE 20. Example computation of T for a wheel with three spokes.

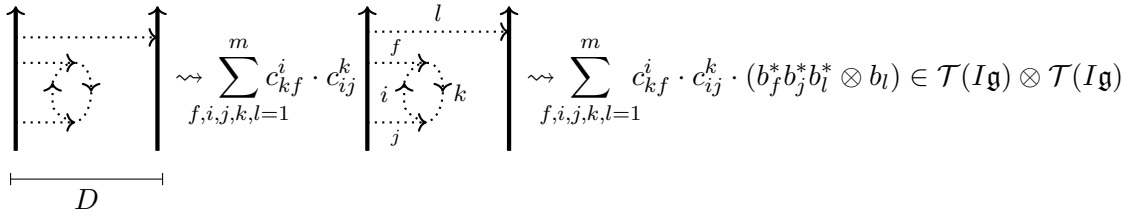

FIGURE 21. An example for computing T.

Proof. We need to check that relations in $\mathcal{A}^w(\uparrow^n)$ are mapped to relations in $(U(I\mathfrak{g})^{\otimes n})$. This is indeed the case: $\overrightarrow{STU}_1$ and $\overrightarrow{STU}_2$ are mapped to the relations $[x_i, x_j] = x_i x_j - x_j x_i$, and $[\varphi_i, x_j] = \varphi_i x_j - x_j \varphi_i$. $\overrightarrow{STU}_3 = TC$ is the fact that $\mathfrak{g}^*$ is abelian. It is also easy to check that the T respects gradings, so the completions on both sides agree. □

Proposition 4.2. *When $k_1+k_2 = n$, T further descends to a well defined map $T : \mathcal{A}^{sw}(\overset{\bullet}{\downarrow}^{k_1}\uparrow^{k_2}) \to \left(S(\mathfrak{g}^*)_{\mathfrak{g}}^{\otimes k_1} \otimes U(\mathfrak{g})^{\otimes k_2}\right)^{\wedge}$.*

Proof. We begin by re-phrasing the statement as a commutative diagram:

$$\begin{array}{ccc} \mathcal{A}(\uparrow^n) & \xrightarrow{\quad T \quad} & \left(U(I\mathfrak{g})^{\otimes k_1} \otimes U(I\mathfrak{g})^{\otimes k_2}\right)^{\wedge} \\ \downarrow & & \downarrow \\ \mathcal{A}^{sw}(\overset{\bullet}{\vdots}{}^{k_1} \uparrow^{k_2}) & \xrightarrow{\exists T} & \left(S(\mathfrak{g}^*)_{\mathfrak{g}}^{\otimes k_1} \otimes U(\mathfrak{g})^{\otimes k_2}\right)^{\wedge} \end{array}$$

The projection on the left is imposing two cap relations on each of the first k_1 strands, and killing all arrow diagrams with any arrow tails on strands k_1+1 through n. One defines the bottom horizontal T map in the obvious way: taking any pre-image on the left, and applying T followed by the quotient on the right. For this to be well-defined, we need to show that any element in the kernel of the projection on the left is killed by the composition of T with the projection on the right.

On strands k_1+1 through n, under the tensor interpretation map T, arrow tails ending on a given strand translate to elements of $\mathfrak{g}^*$ in a product in the corresponding $U(I\mathfrak{g})$ tensor factor. Hence the quotient map to make the bottom arrow well-defined is to set elements of $\mathfrak{g}^*$ to be zero, resulting in the $U\mathfrak{g}$ tensor factors.

On the first k_1 strands, the cap relations assert that an arrow head at the very beginning or the very end of the strand is zero. T assigns elements of $\mathfrak{g}$ to arrow heads, hence, the corresponding quotient map on the right is modding out by the multiplication action of $\mathfrak{g}$ on $U(I\mathfrak{g})$, both on the left and on the right: denote this by $\mathfrak{g}\backslash U(I\mathfrak{g})/\mathfrak{g}$. We only need to prove, then, that $\mathfrak{g}\backslash U(I\mathfrak{g})/\mathfrak{g} \cong (S\mathfrak{g}^*)_{\mathfrak{g}}$.

By the Poincare–Birkhoff–Witt (PBW) theorem, $U(I\mathfrak{g})$ has a linear basis, where each basis element is of the form $(b_1^*)^{\alpha_1}...(b_m^*)^{\alpha_m} b_1^{\beta_1}...b_m^{\beta_m}$, for non-negative integers α_i and β_i, $i = 1...m$. Thus, $U(I\mathfrak{g})/\mathfrak{g} \cong S\mathfrak{g}^*$, as basis elements where $\beta_i \neq 0$ for any i are sent to zero, and g^* is abelian. It remains to show that left multiplication by $\mathfrak{g}$ translates to the co-adjoint action of $\mathfrak{g}$ on $S\mathfrak{g}^*$ under this isomorphism. Given a monomial $b_{i_1}^*...b_{i_r}^* \in S\mathfrak{g}^*$, where $1 \leq i_1 \leq i_2 \leq ... \leq i_r \leq m$, and $b_i \in \mathfrak{g}$, we need to write $b_i b_{i_1}^*...b_{i_r}^*$ in terms of the PBW basis, that is, we need to commute b_i across each of the dual basis elements.

According to the formula (4.1), denoting the coadjoint action of g on φ by $g \cdot \varphi$,

$$b_i b_{i_1}^*...b_{i_r}^* = (b_i \cdot b_{i_1}^*)...b_{i_r}^* + b_{i_1}^*(b_i \cdot b_{i_2}^*)...b_{i_r}^* + b_{i_1}^*...(b_i \cdot b_{i_r}^*) + b_{i_1}^*...b_{i_r}^* b_i = b_i \cdot (b_i b_{i_1}^*...b_{i_r}^*).$$

The second equality holds because last term of the sum in the middle is zero in $U(I\mathfrak{g})/\mathfrak{g}$. Thus, we have shown that $\mathfrak{g}\backslash U(I\mathfrak{g})/\mathfrak{g} \cong (S\mathfrak{g}^*)_{\mathfrak{g}}$, and completing the proof. □

The following Proposition will play a crucial role later; we present it here as it is based on a similar principle as the proof above:

Proposition 4.3. *The image of T is $\mathfrak{g}$-invariant, where $\mathfrak{g}$ acts via the adjoint action on the each of the $U\mathfrak{g}$ tensor factors (that is, sum over acting on each one). In other words, $T(D) \in \left(\left((S\mathfrak{g}^*)_{\mathfrak{g}}^{\otimes k_1} \otimes (U\mathfrak{g})^{\otimes k_2}\right)^{\wedge}\right)^{\mathfrak{g}}$ for any $D \in \mathcal{A}^{sw}(\overset{\bullet}{\vdots}{}^{k_1} \uparrow^{k_2})$.*

Proof. This follows from the *head invariance* property of arrow diagrams: the relevant implication of this fact is shown in Figure 22; the property in general is discussed in [BD2, Remark 3.14]. In short, the sum over all thin red strands of attaching an additional arrow head at the bottom of the strand gives the same result as the sum over all thin red strands of attaching the arrow head at the top.

Attach an additional arrow head at the bottom of the i-th red strand of an arrow diagram D, where the arrow tail lies on an additional strand as in Figure 22; call this new diagram

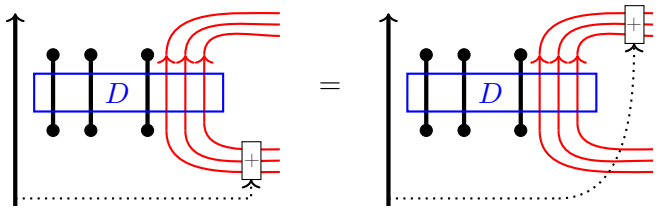

FIGURE 22. The *head invariance* property in $\mathcal{A}^{sw}(\uparrow^{k_1}\uparrow^{k_2})$.

D_i. Compare $T(D_i)$ with $T(D)$:

$$T(D_i) = \sum_{j=1}^{m} b_j^* \otimes (b_j \times_i T(D)),$$

where $\times_i$ denotes multiplying on the left in the i-th tensor factor.

Similarly, let D^i denote the arrow diagram obtained from D by attaching an arrow head at the top of the i-th red strand.

$$T(D^i) = \sum_{j=1}^{m} b_j^* \otimes (T(D) \times_i b_j),$$

where multiplication is now on the right. Hence,

$$T(D_i) - T(D^i) = \sum_{j=1}^{m} b_j^* \otimes (b_j \cdot_i T(D)),$$

where $\cdot_i$ denotes the adjoint action on the i-th $U\mathfrak{g}$ tensor factor. Due to the head invariance property we have

$$0 = \sum_{i=1}^{k_2} T(D_i) - T(D^i) = \sum_{j=1}^{m} b_j^* \otimes \left(\sum_{i=1}^{k_2} b_j \cdot_i T(D) \right).$$

The right hand side is only zero if $\sum_{i=1}^{k_2} b_j \cdot_i T(D) = 0$ for each $j = 1...m$, which is exactly the statement of the proposition. □

4.2. **The tensor statement.** To obtain the tensor statement, we simply apply the map T to the diagrammatic statement of Figure 17:

$$Z\left(\theta\right) \# Z\left(\theta\right) = u^2 Z\left(\theta\right).$$

Since $Z(\theta)$ is an element of $\mathcal{A}^{sw}(\uparrow\uparrow)$, $T(Z(\theta)) =: \Upsilon \in (S(\mathfrak{g}^*)_{\mathfrak{g}} \otimes U(\mathfrak{g}))^\wedge$.

The connected sum operation in $\mathcal{A}^{sw}$ is concatenation along the red strings. Under the tensor interpretation map T, this translates to multiplication in $U(\mathfrak{g})$, while the $S(\mathfrak{g}^*)$ components remain separate tensor factors. Hence,

$$T\left(Z(\theta)\#Z(\theta)\right) = \Upsilon^{13}\Upsilon^{23} \in (S(\mathfrak{g}^*)_{\mathfrak{g}}^{\otimes 2} \otimes U(\mathfrak{g}))^\wedge.$$

Here $\Upsilon^{13} := \phi^{13}(\Upsilon)$, where $\phi^{13}(x \otimes y) := x \otimes 1 \otimes y$, and $\Upsilon^{23} := \phi^{23}(\Upsilon)$, where $\phi^{23}(x \otimes y) := 1 \otimes x \otimes y$.

On the right side, the unzip operation sends an arrow ending on the unzipped strand to a sum of two arrows ending on either daughter strand. Under the tensor interpretation map

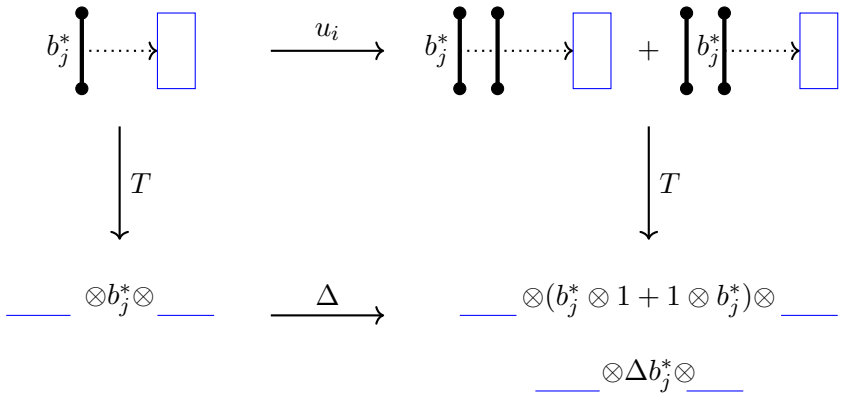

FIGURE 23. The tensor interpretation map intertwines unzip with co-multiplication.

T, this is sent to the Hopf algebra coproduct Δ of $\hat{S}(\mathfrak{g}^*)_{\mathfrak{g}}$ given by $\Delta(\varphi) = \varphi \otimes 1 + 1 \otimes \varphi$ for primitive elements $\varphi \in \mathfrak{g}^*_{\mathfrak{g}}$, as shown in Figure 23. In other words, $T \circ u = \Delta \circ T$, and therefore

$$T\left(u^2 Z\left(\text{-}\right)\right) = (\Delta \otimes 1)\Upsilon \in (S(\mathfrak{g}^*)_{\mathfrak{g}}^{\otimes 2} \otimes U(\mathfrak{g}))^{\wedge}.$$

In summary, we obtain the Tensor Statement::

Tensor Statement

$$\Upsilon^{13}\Upsilon^{23} = (\Delta \otimes 1)\Upsilon \quad \text{in} \quad (S(\mathfrak{g}^*)_{\mathfrak{g}}^{\otimes 2} \otimes U(\mathfrak{g}))^{\wedge}$$

FIGURE 24. The tensor statement.

5. The Duflo Isomorphism

There is a pairing $\mathfrak{g}^* \times \mathfrak{g} \to \mathbb{K}$ given by the evaluation. This extends to a pairing $S\mathfrak{g}^* \times S\mathfrak{g} \to \mathbb{K}$ in the following way. Given a monomial $\varphi_1 \cdot ... \cdot \varphi_k \in S\mathfrak{g}^*$ with $\varphi_i \in \mathfrak{g}^*$ and a monomial of the same degree $x_1 \cdot ... \cdot x_k \in S\mathfrak{g}$ with $x_j \in \mathfrak{g}$,

$$\langle \varphi_1 \cdot ... \cdot \varphi_k, x_1 \cdot ... \cdot x_k \rangle := \sum_{\sigma \in S_k} \varphi_1(x_{\sigma(1)}) \cdot ... \cdot \varphi_k(x_{\sigma(k)}), \tag{5.1}$$

where the sum is over all permutations of the k indices. Monomials pair as zero with any monomial of a different degree, and the pairing is then extended bilinearly.

Alternatively, given a basis $\{b_1, ..., b_m\}$ of $\mathfrak{g}$ and dual basis $\{b_1^*, ..., b_m^*\}$ of $\mathfrak{g}^*$, $S\mathfrak{g}$ and $S\mathfrak{g}^*$ are spanned linearly by monomials in the basis elements b_i and b_j^* respectively. The monomial $(b_1^*)^{\alpha_1} \cdot ... \cdot (b_m^*)^{\alpha_m}$ pairs as zero with every monomial in the basis vectors $\{b_i\}$ except $b_1^{\alpha_1} \cdot ... \cdot b_m^{\alpha_m}$,

and

$$((b_1^*)^{\alpha_1}\cdot\ldots\cdot(b_m^*)^{\alpha_m})\Big(b_1^{\alpha_1}\cdot\ldots\cdot b_m^{\alpha_m}\Big)=\prod_{i=1}^m\alpha_i! \tag{5.2}$$

This descends to a pairing $(Sg^*)_{\mathfrak{g}}\times(S\mathfrak{g})^{\mathfrak{g}}\to\mathbb{K}$. For $\Pi\in(Sg^*)_{\mathfrak{g}}$ and $P\in(S\mathfrak{g})^{\mathfrak{g}}$ we will denote the value of this pairing by by $\langle\Pi,P\rangle$. Finally, one can extend to a pairing $(Sg^*)_{\mathfrak{g}}^{\otimes n}\times((S\mathfrak{g})^{\mathfrak{g}})^{\otimes n}\to\mathbb{K}$ by simply multiplying the pairings of tensor factors. This satisfies the equality

$$\langle\Pi,PQ\rangle=\langle\Delta\Pi,P\otimes Q\rangle \tag{5.3}$$

for any $P,Q\in(S\mathfrak{g})^{\mathfrak{g}}$, where Δ is the co-product on $(Sg^*)_{\mathfrak{g}}$ induced by the co-product on Sg^*.

Define the Duflo map

$$\mathcal{D}:S(\mathfrak{g})^{\mathfrak{g}}\to U(\mathfrak{g})^{\mathfrak{g}}$$

by pairing with the first tensor factor of $\Upsilon\in(S(\mathfrak{g}^*)_{\mathfrak{g}}\otimes U(\mathfrak{g}))^\wedge$, and by an abuse of notation, denote this by $\mathcal{D}(P)=\langle\Upsilon,P\rangle$. Note that although Υ lives in a degree completion, it is finite in each degree, and so only finitely many terms of Υ have non-zero pairings with any given $P\in S(\mathfrak{g})^{\mathfrak{g}}$. Hence, $\mathcal{D}(P)\in U(\mathfrak{g})$. The fact that $\mathcal{D}(P)$ is $\mathfrak{g}$-invariant is a direct consequence of Proposition 4.3.

Theorem 5.1. *The map $\mathcal{D}$ is an algebra homomorphism.*

Proof. By definition, $\mathcal{D}$ is linear. The multiplicativity of $\mathcal{D}$, on the other hand, is a direct consequence of the Tensor Statement. Let $P,Q\in S(\mathfrak{g})^{\mathfrak{g}}$, then

$$\mathcal{D}(PQ)=\langle\Upsilon,PQ\rangle\overset{1}{=}\langle(\Delta\otimes1)\Upsilon,P\otimes Q\rangle\overset{2}{=}\langle\Upsilon^{13}\Upsilon^{23},P\otimes Q\rangle\overset{3}{=}\mathcal{D}(P)\mathcal{D}(Q).$$

Here Equality 1 is Equation (5.3) above, and the second pairing is applied in the first two tensor factors of $(\Delta\otimes1)\Upsilon$. Equality 2 is the Tensor Statement, and the pairing is still applied to the first two tensor factors of the first argument. Equality 3 is simply the associativity of product. □

Proposition 5.2. *The map $\mathcal{D}$ is an algebra isomorphism.*

Proof. In light of Theorem 5.1 we only need to prove that $\mathcal{D}$ is bijective. Recall that $U\mathfrak{g}$ is filtered by word length (aka the PBW filtration), and the PBW Theorem states that the associated graded algebra is isomorphic to $S\mathfrak{g}$. We claim that $\mathcal{D}$ is a filtered map; this is true by inspection of Υ as below. We then prove that $\operatorname{gr}\mathcal{D}$ is the identity, hence $\mathcal{D}$ is bijective.

Recall that $Z(\text{-}\vert\text{-})$ consists of a value C^2 on the twice-capped strand followed by an exponential e^a of an arrow a from the capped startand to the red string, as shown in Figure 17. Hence,

$$T(Z(\text{-}\vert\text{-}))=(T(C^2)\otimes1)\cdot T(e^a).$$

Since $T(a)=\iota$, where $\iota\in\mathfrak{g}^*\otimes\mathfrak{g}$ denotes the structure tensor of the identity automorphism of $\mathfrak{g}$, we have $T(e^a)=e^\iota$. Recall from Formula (3.1) that $T(C^2)=1+\text{higher degree terms}$.

Now let $P\in S(\mathfrak{g})^{\mathfrak{g}}$ be homogeneous of degree d. Observe that $\mathcal{D}(P)$ lives in filtered degree *at most* d, hence $\mathcal{D}$ is a filtered map. In particular the only term of $\mathcal{D}(P)$ that doesn't belong to filtered degree $d-1$ arises from pairing with $\frac{1}{d!}\iota^d$.

Hence, the associated graded map $\operatorname{gr}\mathcal{D}(P)=\operatorname{gr}(P\mapsto\langle e^\iota,P\rangle)$, and by formula (5.1) this is the identity of $S\mathfrak{g}$, completing the proof. □

References

[AM] A. Alekseev and E. Meinrenken, *On the Kashiwara-Vergne conjecture,* Inventiones Mathematicae, **164** (2006) 615–634, arXiv:0506499.

[AET] A. Alekseev, B. Enriquez, and C. Torossian, *Drinfeld's associators, braid groups and an explicit solution of the Kashiwara-Vergne equations,* Publications Mathématiques de L'IHÉS, **112-1** (2010) 143–189, arXiv:0903.4067.

[AT] A. Alekseev and C. Torossian, *The Kashiwara-Vergne conjecture and Drinfeld's associators,* Annals of Mathematics **175** (2012) 415–463, arXiv:0802.4300.

[BD1] D. Bar-Natan and Z. Dancso, *Finite Type Invariants of W-Knotted Objects I: W-Knots and the Alexander Polynomial,* Alg. Geom. Topol. **16** (2016) 1063–1133.

[BD2] D. Bar-Natan and Z. Dancso, *Finite Type Invariants of W-Knotted Objects II: Tangles and the Kashiwara-Vergne Problem,* Math. Annalen **367**(3-4) (2017) 1517–1586. arXiv:1405.1955.

[BD3] *Finite Type Invariants of W-Knotted Objects III: the Double Tree Construction* draft.

[BLT] D. Bar-Natan, T. Q. T. Le, and D. P. Thurston, *Two applications of elementary knot theory to Lie algebras and Vassiliev invariants,* Geom. Topol. **7-1** (2003) 1–31, arXiv: math.QA/0204311.

[BH] T. Brendle and A. Hatcher, Configuration Spaces of Rings and Wickets, Comment. Math. Helv. **88** (2013), no. 1, 131–162. arXiv:0805.4354

[CS] J. S. Carter and M. Saito, *Knotted surfaces and their diagrams,* Mathematical Surveys and Monographs **55**, American Mathematical Society, Providence 1998.

[D] M. Duflo, *Opérateurs différentiels bi-invariants sur un groupe de Lie*, Ann. Sci. École Norm. Sup. **10** (1977), 265–225.

[Gol] D. M. Goldsmith, *The Theory of Motion Groups,* Mich. Math. J. **28-1** (1981) 3-17.

[HC] Harish-Chandra, *On Some Applications of the Universal Enveloping Algebra of a Semisimple Lie Algebra* Trans. Amer. Math. Soc. **70** (1951), 28–96.

[J] V. F. R. Jones, *Planar algebras I*, arXiv:math/9909027

[KV] M. Kashiwara and M. Vergne, *The Campbell-Hausdorff Formula and Invariant Hyperfunctions,* Invent. Math. **47** (1978) 249–272.

[Sa] S. Satoh, *Virtual Knot Presentations of Ribbon Torus Knots*, J. Knot Theory Ramifications **9-4** (2000) 531–542.

Department of Mathematics, University of Toronto, Toronto Ontario M5S 2E4, Canada
Email address: drorbn@math.toronto.edu
URL: http://www.math.toronto.edu/~drorbn

Mathematical Sciences Institute, Australian National University, John Dedman Bldg 26, Acton ACT 2601, Australia
Email address: zsuzsanna.dancso@anu.edu.au
URL: http://www.math.toronto.edu/zsuzsi

Department of Mathematics, South Hall, Room 6607, University of California, Santa Barbara, CA 93106-3080, United States
Email address: nscherich@math.ucsb.edu
URL: http://www.nancyscherich.com